Unsteady Measurements for a Periodically Plunging Airfoil

N. Chiereghin[1], D. J. Cleaver[2] and I. Gursul[3]
University of Bath, Bath, England BA2 7AY, United Kingdom

The fluid dynamics of wings under extreme gusts, oscillations and maneuvers is an area of current research interest. For civil aircraft, a more accurate prediction of the loads in extreme condition is required to reduce uncertainty and facilitate a more efficient structural design of the wing. Unsteady force and particle image velocimetry measurements are performed on a plunging airfoil at a low Reynolds number of Re=20,000 for a range of normalized amplitude from 0.05 to 0.5, reduced frequency from 0 to 0.95 and angles of attack from 0° to 15°. Results are compared to the classical Theodorsen model predictions. Good agreement is observed between theoretical and experimental results for the amplitude of lift fluctuation even for high frequencies and angles of attack. An overall good agreement is also observed between measured and predicted phase lag. This agreement of amplitude and phase lag is surprising given the vortical structures observed in the phase-averaged velocity field, which should invalidate the Theodorsen model. However, the measured time-averaged lift is substantially different from both the measured static and the theoretical values. In contrast with Theodorsen prediction, the time-average lift has a strong dependence on plunging frequency and amplitude when the effective angle of attack approaches or exceeds the stall angle. Flow field measurements show that this variation of mean lift is related to the intensity of the leading edge vortex.

Nomenclature

A	=	peak-to-peak amplitude, $2a$
a	=	plunging amplitude
a_0	=	time-averaged lift
a_1	=	first harmonic of lift oscillation
b	=	wing spanwise length
c	=	chord
C_l	=	lift coefficient, $l/0.5\rho U_\infty^2 cb$
f	=	frequency
FFT	=	fast Fourier transform
h	=	plunging motion coordinate
k	=	reduced frequency, πSr_c
l	=	lift force
M_x	=	bending moment
M_z	=	pitching moment
Re	=	Reynolds number,
Sr_c	=	Strouhal number based on chord, fc/U_∞
T	=	plunge period
U_{pl}	=	plunge velocity
U_∞	=	freestream velocity
α	=	geometric angle of attack

---

[1] Research Associate, Department of Mechanical Engineering.
[2] Lecturer, Department of Mechanical Engineering, Member AIAA.
[3] Professor, Department of Mechanical Engineering, Associate Fellow AIAA.

α_{eff} =   effective of attack, $\alpha + \tan^{-1}\left(U_{pl}/U_\infty\right)$

Φ =   phase lag

I. Introduction

UNSTEADY aerodynamics of plunging airfoils has received substantial interest for its numerous applications, which includes helicopters blades [1], micro air vehicles [2] and aircraft wing load during turbulence and gusts [3]. Previous measurements for small-amplitude oscillating airfoils [4] demonstrated substantial increase in spanwise cross-correlation coherency for a range of plunging Strouhal number in the range Sr_c=0.2-1.2. This is in contrast to static conditions where stall is characterized by massive separation with low spanwise coherency. Flow field measurements showed that this coherency is related to spanwise coherent structures like leading-edge and trailing edge vortices. The increase in coherency is also associated with a remarkable increase in time-averaged lift [4,5].

The increase in time-averaged lift is considered a benefit for applications like micro vehicles. Conversely, a large increase in unsteady lift during gust encounters or extreme manoeuvers, even for a short time, can have a detrimental effect on the stability and structural integrity of civil aircraft. It is therefore necessary to have a model capable of predicting peak loads during these extreme conditions. Current numerical methods are characterized by poor confidence in predicting unsteady loads or require unrealistic computational resources for extreme flight conditions. As a consequence, high safety factors are applied during the design process. Since these extreme cases dictates the structural requirements, this produces a substantial increase in the design, manufacturing and operational cost.

Currently, the Theodorsen model [6] is the most commonly used method for the prediction of the lift variation over a plunging airfoil. This model is based on the attached and irrotational flow hypotheses and is defined for small sinusoidal oscillations of the airfoil. Both plunging (vertical) and pitching oscillations are included in this theory. Under these conditions an exact formula is derived for fast calculation of lift and pitching moment without numerical integration or empirical coefficients. Theodorsen theory takes into account the periodic variation of the effective angle of attack (as in the quasi-static approach) together with the effect of the wake and the acceleration of the flow around the airfoil. For an angle of attack of 0° Halfman [7] observed good agreement with experimental data for a range of reduced frequency from 0 to 0.4 and peak-to-peak amplitude of $0.15c$ and $0.3c$. In Mertens *et al.* [8] good agreement was observed with measurements and CFD at a geometric angle of attack of 10°, but increasing the angle to 12° resulted in some disagreement. Obviously, Theodorsen model is not suitable for quantifying the effect of flow separation where vortical structures are generated. To overcome this limitation a number of models have been developed that take into account the effect of dynamic separation for high angles of attack [9]. For the Leishman-Beddoes model good agreement with experimental data was reported [10] for airfoil oscillations around stall angle for reduced frequency around 0.1. However, these models are semi-empirical and require coefficients which makes them less robust. It is therefore not possible to extend their application beyond the range of their calibrated frequency and amplitude. In the current paper we will be applying relatively large reduced frequencies and effective angle of attack amplitudes that exceed this applicable range. More recently new approaches based on discrete vortex methods have been proposed [11]. These methods are more suitable to quantify the suction effect of coherent structures [4] but are more complex to implement than Theodorsen formula and require numerical integration.

In this paper Theodorsen theory is tested for a plunging airfoil (see Fig. 1) in a range of amplitude, reduced frequency and angle of attack that covers the gust range of civil aircraft. Theodorsen predictions are compared with measured lift in terms of time-average, amplitude and phase lag. Particle image velocimetry measurements are conducted to assess the effect of frequency and geometric angle of attack on the velocity field around the airfoil, with focus on the low pressure side where spanwise coherent vortical structures are expected [12].

II. Experimental Method

Unsteady lift and phase-averaged PIV measurements were conducted at Re=20,000 for a NACA0012 airfoil plunging with sinusoidal motion normal to the freestream flow direction, see Figure 1. Four different geometric angles of attack were tested, i.e., α=0°, 5°, 9°, 15°. These were selected to be representative of the symmetry (0°), pre-stall (5°), stall (9°) and post-stall cases (15°). Unsteady and phase-averaged measurements are conducted with sinusoidal plunging motion with a range of reduced frequency k from 0.0 to 0.95 (Sr_c=0.3) and peak-to-peak amplitude range of A/c = 0.05, 0.1, 0.3, 0.5. This covers the gust range reported in CS-25 [3].

American Institute of Aeronautics and Astronautics

A. Experimental Setup

The experiments were performed in the close-loop free surface water tunnel facility at the University of Bath. The water tunnel has a glass working section with dimensions 381 x 508 x 1530 mm. The flow speed range covers from 0 to 0.5 m/s with a turbulence intensity of less than 0.5% [13].

The wing is vertically mounted to a linear motion mechanism, as shown in Figure 2. The wing has a NACA0012 profile with a chord of 62.7 mm with an aspect ratio of 5.It is manufactured through selective laser sintering (SLS) with a polished smooth surface. Inside the wing a 25x5 mm rectangular bar of T800 carbon fiber is inserted for high spanwise stiffness. In order to prevent the tip vortex and spanwise flow, a carbon fiber plate was fixed to the root of the wing, and a glass plate was placed at the tip with a clearance of 2 mm (Figure 2). This design ensures quasi-2D airfoil measurements. The wing in connected to a moving platform through a rotation stage which allows variation of the geometric angle of attack with an accuracy of ±0.2°. The moving platform is connected to a fixed frame with four air-bearings that absorb the bending and torque loads whilst enabling frictionless motion. The plunging motion was supplied by a Zaber LSQ150B-T3 translation stage powered by a stepper motor with an X-MCB1 controller. The plunging motion follows a sinusoidal function with an accuracy of 2%.

B. Load measurements

The force measurement system is used to acquire lift, bending and pitching moment in both static and dynamic conditions. An S-beam load cell is placed between the moving platform and the motorized translation stage to measure the lift along the plunging direction, i.e. normal to the freestream flow direction. A moment sensor is placed between the moving platform and the wing to measure bending moment, i.e. the moment vector component parallel to the freestream direction. This report focuses on two-dimensional airfoil measurement, therefore the bending moment is used for validation as a second measurement of lift under the assumption of two-dimensional flow, i.e., $l = M_x/0.5b$.

The static measurements are acquired for 60 seconds at data acquisition rate (DAQ) rate of 1 kHz. For dynamic measurements the DAQ rate is set to 2,000 times the plunging frequency and is acquired for 55 plunging periods. The first five periods are excluded from the analysis. From dynamic measurements the time-average a_0, first harmonic amplitude a_1 and phase lag Φ of lift oscillation are extracted. The first harmonic a_1 represents the amplitude of the plunging frequency component of the Fourier Transform of the lift signal. Phase lag is the phase difference between the first harmonic of the lift signal and the plunging motion signal. The original lift signal includes inertia of the moving components like the wing and moving platform. In order to remove this component, measurements are also taken in air. The fast Fourier transform is calculated for both the air and flow test. The first harmonic component of the spectrum of the air test is then subtracted from the first harmonic of the flow test. The module of this subtraction represents the first harmonic amplitude a_1, while its phase represents the phase lag Φ between plunging motion and lift signal. The averaged lift a_0 is simply the time-average of the lift signal. The phase-average is calculated over 50 periods for each vertical position of the airfoil during the plunging motion and is defined as a function of t/T, the elapsed time relative to the period (Figure 1). The uncertainty in the measurement of lift coefficient C_l is estimated to be ±0.05 for static measurements and ±0.10 for dynamic measurements.

C. Theoretical model

Currently, the most broadly used method for estimating unsteady loads is the Theodorsen theory [1,6], which gives a simple solution to predict the loads of a 2D harmonically oscillating airfoil under the assumptions of inviscid, incompressible flow and small oscillations. Equation 1 is the Theodorsen formula to estimate the lift coefficient of harmonic vertical plunging motion, $h(t) = ae^{j2\pi ft}$.

$$C_l = [2\pi kjC(k) - \pi k^2]\frac{A}{c}e^{j2\pi ft} + 2\pi C(0)\alpha \qquad (1)$$

The right side contains a harmonic and a static term. The harmonic term contains a circulatory part $2\pi kjC(k)$, which is dominant for low reduced frequency, and an added-mass part πk^2, which becomes dominant at high reduced frequency. The Theodorsen's function C(k) is a complex term based on the effects of the shed wake and its module starts from unity for k=0 and monotonically converges to about 0.5 for k=∞. The static term determines the time-averaged value of the lift. In this case the value of the Theodorsen function C is determined by the frequency of the oscillation of the geometric angle of attack, which is maintained fixed during the plunging motion in this study.

American Institute of Aeronautics and Astronautics

Therefore, for pure vertical oscillations of the airfoil C=1 for each frequency and amplitude, and the predicted time-averaged lift coincides with the thin airfoil linear theory prediction $2\pi\alpha$.

D. Particle Image Velocimetry

Two-dimensional PIV measurements are taken in a cross-section in the central spanwise plane of the wing, as shown in Figure 2b. The laser is positioned to the side of the working section, while a camera views the region of interest from below. The low pressure side of the airfoil is illuminated with a Nd:YAG 50 mJ pulsed laser. The image is captured with a twelve bit charge-coupled device camera of 4 mega pixel. The water tunnel was seeded with hollow glass particle with size of 8-12 µm.

Phase-averaged flow field measurements of the velocity field were conducted at interval of 1/8 of the plunging period combining a TSI synchronization system with a Renishaw optical linear encoder. Phase-averaged data are derived from 100 image pairs. The camera was focused on a region from 0.3c upstream of the airfoil to 0.8c downstream. The images were processed using the software Insight 4G with an interrogation window of 48x48 pixels and a grid overlap of 0.25 giving a spatial resolution of about 1% of the wing chord.

III.   Results

In part A and B the analysis covers the impact of plunging frequency and amplitude on time-averaged lift, module of the first harmonic of lift and phase lag of lift for different geometric angles of attack. The experimental results are compared with the predictions of the Theodorsen model [6]. In part C the phase averaged velocity field is analyzed to identify the major spanwise vortical structures and assess their impact on the phase-averaged lift.

A. Time-Averaged Lift

The time-averaged lift in static conditions is presented in Figure 3. In order to validate the measurement system time-averaged lift measurements from the S-beam load cell are compared with measurements from the moment sensor and with measurements from the literature. There is a good agreement between the two instruments, which also demonstrates that the time-averaged flow field is substantially two-dimensional. There is also excellent agreement with the published measurements from Cleaver *et al.*[14]. The lift measurements in Cleaver *et al.* [14] have previously been validated against other sources [15, 16]. The $2\pi\alpha$ straight line derived from the thin airfoil linear theory coincides with the mean lift predicted by the Theodorsen model for a pure vertically plunging airfoil (Equation 1). As expected the measured lift is close to $2\pi\alpha$ until the stall angle of 9°. A reduced slope of the measured C_l curve is observed for α<3°. This appears to be related to the curvature of the leading-edge of the airfoil profile at low Reynolds numbers. Indeed, this characteristic is also observed [17,18] for a NACA0012 but not for a plate with low camber. It is evident for Re<30,000 and disappears for Re higher than 70,000 [18]. Moreover, this effect is not observed if the NACA0012 is reversed [18].

For the plunging airfoil, the measured time-averaged lift is presented in Figure 4 as a function of angle of attack, plunging amplitude and reduced frequency. For α=0° time-averaged lift is approximately zero for all reduced frequencies as dictated by symmetry, as seen in Figure 4a. It is only at very high plunge velocities that one observes symmetry breaking [12].

At the pre-stall angle α=5° (Figure 4b) time-averaged lift converges to the static value at low frequency as expected, and remains almost constant for plunging amplitude A/c of 0.05 and 0.1 across the frequency range considered. For amplitude A/c of 0.3 and 0.5, initially there is a small reduction of the time-averaged lift as reduced frequency increases, followed by an inversion of the trend so that time-averaged lift increases as reduced frequency k approaches unity. With A/c=0.5 the time average lift exceeds the static value when k>0.6, with an increase of 20% at the maximum frequency k=0.95. For this angle of attack the Theodorsen prediction based on the $2\pi\alpha$ curve is close to the measured time-averaged lift because of the attached flow (Figure 3). However, the dependency on the plunging frequency of time-averaged lift is not predicted by the Theoretical model (Equation 1).

When the angle of attack is increased to the stall angle α=9° (Figure 4c) the dependency on the frequency is more pronounced. The time-averaged lift increases almost monotonically with reduced frequency for k>0.2 for all plunging amplitudes. Similar to α=5°, the slope of the A/c=0.5 curve increases at k=0.6. The maximum increase in time-averaged lift at k≈0.95 is now 50% of the static value.

At the post-stall angle of 15° (Figure 4d) the dependency on frequency and plunging amplitude is further amplified. For A/c=0.5, there is a rapid increase of time-averaged lift between k≈0.1 and 0.3. Then the trend remains almost constant until 0.6. Similar to the other angles of attack, the lift trend has a sudden increase of the slope at k≈0.6. At the maximum frequency considered the time-averaged lift reaches a value 150% higher than the static value. As the plunging amplitude is reduced to 0.3, the increase in lift is delayed to k≈0.2. It is interesting to note that both A/c=0.3 and 0.5 exhibit a 'plateau' region of constant lift in the middle of the frequency range analyzed, with the same value of time-averaged lift and a similar frequency extent, although the plateau for the lower amplitude is at a higher frequency. After the plateau the trend at A/c=0.3 has a rapid increase but with a gradient lower than the A/c=0.5 curve. As the amplitude is decreased to A/c=0.1 and 0.05, there is still a monotonic increase of lift with frequency but with a lower gradient and the plateau is not visible in the frequency range k=0 to 0.95. These measurements are in agreement with previous measurements for a NACA 0012 airfoil at α=15° [4] that showed an approximately linear increase in time-averaged lift with plunge velocity. The linear theory is not valid at post-stall angles of attack, as seen in Figure 3 and therefore is in poor agreement even at k=0. Furthermore, the strong dependence on the frequency of the time-averaged lift is in stark contrast with the classical formulation of the Theodorsen theory.

B. Lift variation

The module of the first harmonic of lift is presented in Figure 5 as a function of angle of attack, plunging amplitude and frequency. For an angle of attack of 0° (Figure 5a) there is excellent agreement between the Theodorsen prediction and experimental measurement even for very high frequencies. There was also excellent agreement for time-average lift which implies the assumptions underlying Theodorsen are still valid at this low angle of attack despite the large effective angles of attack. Surprisingly, there is a very good agreement between measurements and Theodorsen prediction for 5° (Figure 5b), even for combinations of high reduced frequency and peak-to-peak amplitude where the model fails to predict the time-averaged lift (Section III.A). Some departure from Theodorsen theory is observed for amplitude measurements at the stall angle (Figure 5c) and post-stall angle 15° (Figure 5d), although the trend is remarkably similar. In general the theoretical trend has a negative curvature for k<0.6 where the circulation is dominant as an effect of Theodorsen's function $C(k)$. For k>0.6 the added-mass force becomes dominant, the lift amplitude gradually becomes a quadratic function of k and the trend gains a positive curvature. This trend is well followed by the experimental measurements at symmetry and pre-stall angles α = 0 and 5°. At the stall angle α = 9° the measured lift amplitude is higher than the Theodorsen prediction for k<0.6 where the lift formula is dominated by the circulation term, which cannot be accurately modelled due to the attached flow assumption. For k>0.6, the Theodorsen prediction follows the measurement better because the dominant added-mass force depends more on the pressure field of the airfoil and less on the flow separation. For post-stall angle α = 15°, the measured values are higher than the model for a broader range of reduced frequency k.

For flight stability assessment and wing structural design it is important to know the peak value of lift during a cycle, which is approximated in Figure 6 as the sum between the time-averaged value a_0 and the amplitude a_1. For a theoretical comparison, since the $2\pi\alpha$ curve is invalid at higher α, the theoretical value is obtained through the sum of the amplitude calculated with Theodorsen model and the measured static lift. In symmetry flow conditions, α = 0° (Figure 6a), the time-averaged lift is approximately zero for the tested range (Figure 4a), so the peak value curves coincide with the amplitude curves in Figure 5a, and the theoretical peak values are in good agreement with the experimental values. The agreement is still good at α = 5°, as seen in Figure 6b. The maximum difference observed is a larger measured value by up to 10% for k>0.6 at the maximum plunging amplitude A/c=0.5. The prediction of the theoretical model becomes less reliable at the stall angle α = 9° (Figure 6c), where the measured peak value exceeds the calculated value by up to the 20%. A higher growth of the lift is observed for post-stall (Figure 6d) angles where the measured peak value exceeds the static value by up to 470%, and exceeds the theoretical value by up to 70%. Comparing the peak value curves with α = 9° and α = 15° (Figure 6c-d), it is noteworthy that the peak lift at α = 9° is 30% higher for low frequencies (k<0.1) but for higher frequencies the trend becomes inverted with peak lift at α = 15° becoming 30% higher than α = 9°. It is inferred that the increase in geometric angle of attack amplifies the increase in time-averaged lift created by the plunging motion.

The phase lag is generally well predicted by Theodorsen theory (Figure 7). There is some disagreement between measurements and theory at low frequency (k<0.2), which is attributed to the uncertainty due to the very small magnitude of lift signal. For k=0 Theodorsen predicts a phase lag Φ≈270°, i.e. the time history of lift has a delay of 90° from the plunge function $h(t)$ in Figure 1. For low reduced frequency the circulation forces are dominant. Circulation forces follow the effective angle of attack, which has a phase approximately opposite to the plunge velocity. As the reduced frequency increases the phase lag moves closer to 360° as the added-mass forces become

5

dominant. The added-mass forces are in opposite phase with the plunge acceleration, and therefore in phase with *h(t)*. In contrast with the time-averaged value and amplitude, the impact of the plunging amplitude *A/c* and geometric angle of attack on phase lag is modest, in particular at high reduced frequency.

C. Phase-averaged measurements
    More insight is gained into the flow physics of the plunging airfoil by considering the phase-averaged distribution of lift during a plunging cycle alongside the phase-averaged velocity field. The effect of the frequency and geometric angle of attack on the phase-averaged lift is outlined in Figures 8 and 9 for *k*=0.47 and 0.94 respectively. The phase-average lift is plotted against the effective angle of attack and is compared with the static lift curve. Also included is the measured lift using just the first harmonic and the Theodorsen function with the time-averaged term of Equation 1, which is based on the linear theory, replaced by the time-averaged lift from dynamic measurements.
    The impact of the geometric angle of attack on the phase-averaged lift is illustrated in Figure 8 for *k*=0.47, which is in the middle of the tested range, for the maximum plunging amplitude *A/c*=0.5. For symmetric conditions (α = 0°) the phase-averaged lift is in good agreement with the Theodorsen prediction, since at this frequency the circulatory part of the lift is still dominant. The amplitude of the lift variation is well predicted by the model, as also shown in Figure 5a. It is noteworthy that there is also very good prediction of the amplitude and slope for α = 5° (Figure 8b) even if the effective angle of attack is higher than the stall angle for almost 40% of the cycle. The cycle exceeds post-stall effective angles of attack for at least 50% of the period when the geometric angle of attack is set to α=9 and 15°. However, even in these cases there is still only minor disagreement between Theodorsen and the measurements. There is only a slight increase of slope in the experimental cycle, in particular for α = 15°, which determines the increase of lift amplitude around *k*=0.5 with respect to the Theodorsen curves shown in Figure 5 c-d. On the other hand, it is observed that the phase-averaged distribution is shifted up from the static curve once the cycle begins to exceed post-stall angles.
    As the reduced frequency increases to *k*=0.94 the added mass force becomes more relevant (Figure 9). The phase-averaged distribution of lift has a strong hysteresis since the added mass is determined by the vertical acceleration of the airfoil. For α = 0° the effective angle of attack oscillates between ±25°. When the geometric angle of attacked is increased to 15° this becomes offset producing a range of α_{eff} = -10° to 40°. Surprisingly, there is a good agreement between the phase-averaged lift and the Theodorsen model for every geometric angle of attack. Hence, the hysteresis of the cycle is well described by the change in phase lag and the amplitude predicted by the Theodorsen model. There is only a modest difference between the phase-averaged distribution and its first harmonic, in particular when the airfoil moves upwards between *t/T*=0.5 and 0.75. This difference increases with the geometric angle of attack. As for the lower frequency case, an effective angle of attack higher than stall angle produces a shift up of the phase-averaged lift cycle.
    The contour of spanwise vorticity from PIV measurements are presented in Figures 10-13 for four different airfoil positions in the plunging cycle (Figure 1). For α = 0° at *k*=0.47 (Figure 10, left column) no significant vortical structure is observed, with only an increase of the boundary layer thickness during the downward movement of the airfoil between *t/T*=0 to 0.5. Since the flow remains irrotational the unsteadiness of the lift follows the Theodorsen model as expected (Figure 8a). When the frequency is increased to *k*=0.94 (Figure 10, right column) the increase of boundary layer thickness between *t/T*=0 to 0.5 is amplified, with localized flow separation around *c*/4 downstream from the leading edge during *t/T*=0.25 to 0.5, where the effective angle of attack is higher than the stall angle. However, no significant vortical structure detaches from the airfoil and the phase-averaged lift closely follows the Theodorsen function (Figure 9a). In comparison with *k*=0.47, there is a broader oscillation of the wake from the trailing edge.
    The increase of the angle of attack to α = 5° shown in Figure 11 has a more noticeable effect of the flow field. For plunging frequency *k*=0.47 an extended separation is generated from *t/T*=0.25 to 0.5. This produces a negligible variation in the time-averaged lift, as seen in Figure 4b. As the frequency is increased to *k*=0.94 the flow separation is converted into a coherent structure generated from the leading edge which propagates downstream over the airfoil upper surface during the plunging cycle. The signature of negative vorticity between vortex and airfoil indicates a strong reversed flow. In contrast with separation this coherent leading edge vortex (LEV) structure produces an increase in time-averaged lift (Figure 4a). The effect of the LEV on the amplitude of the lift variation is however small. As the angle of attack is increased to α = 9° (Figure 12), the LEV increases in intensity and strength and the coherent structure is now visible also at the moderate frequency of *k*=0.47. Such an increase of vorticity on the upper surface of the airfoil has little effect on the shape of the phase-averaged lift cycle (Figure 9c). However, the effect of the LEV is evident in the increase of the time-averaged lift as shown in Figure 4c. This effect is further compounded for the post stall angle of attack α = 15°. In this case the size and strength of the LEV is further increased and the time-

6

American Institute of Aeronautics and Astronautics

averaged lift is significantly increased (Figure 4d). Note that the increase in strength of the LEV from $\alpha = 9°$ to $15°$ makes the time-averaged lift of the latter higher even though the static lift at $15°$ is lower. However the effect on the amplitude is not as remarkable. It is inferred that at high frequency the cyclic variation is dominated by the added mass force which is proportional to the square of the frequency. This makes the Theodorsen model still reliable to predict the amplitude of the lift periodical oscillation even at reduced frequency $k \approx 1$, where strong coherent vortical structures invalidate the irrotational flow hypothesis underlying the Theodorsen theory. Conversely, the LEV produces a strong increase in time-averaged lift with respect to the static value that the Theodorsen theory cannot predict. Alternative methods are therefore required.

IV. Conclusions

Unsteady load measurements are used to investigate the capability of Theodorsen theory to predict the unsteady lift of an airfoil during plunging motions at moderate to high effective angles of attack. Theodorsen model is capable of predicting lift amplitude for pre-stall geometric angle of attack, with some minor differences for stall and post stall. It is capable of predicting the phase of the first harmonic for all angles with a good degree of accuracy. With regards to the time-averaged loads, Theodorsen theory is not able to predict the substantial increase of lift when the plunging frequency increases, even for pre-stall geometric angles of attack. Flow field measurements reveal that the time-averaged lift increase is associated with the formation of a spanwise leading edge vortex. This coherent structure appears at high frequency but has low impact on the amplitude of lift unsteadiness because at high plunging frequency the added-mass force dominates relative to circulation. To accurately predict the unsteady forces at these high effective angles of attack will require a model that takes into account this mean offset.

Acknowledgments

[1] Leishman, J. G., *Principles of Helicopter Aerodynamics*, 2nd ed., Cambridge University Press, 2006, chap. 8.

[2] Mueller, T. J., and DeLaurier, J. D., "Aerodynamics of Small Vehicles," *Annual Review of Fluid Mechanics*, vol. 35, 2003, pp. 89-111. doi: 10.1146/annurev.fluid.35.101101.161102

[3] European Aviation Safety Agency, "Certification Specifications and Acceptable Means of Compliance for Large Aeroplanes,", CS-25, 2015.

[4] Cleaver, D. J., Wang, Z., Gursul, I., and Visbal, M. R., "Lift Enhancement by Means of Small-Amplitude Airfoil," *AIAA Journal,* vol. 49, no. 9, 2011, pp. 2018-2033. doi: http://dx.doi.org/10.2514/1.J051014

[5] Calderon, D., Wang, Z. , Gursul I., and Visbal, M. R., "Volumetric measurements and simulations of the vortex structures generated by low aspect ratio plunging wings," *Physics of Fluids ,* vol. 25, No. 6, 2013. doi:http://dx.doi.org/10.1063/1.4808440

[6] Theodorsen, T., "General Theory of Aerodynamic Instability and the Mechanics of Flutter," NACA Rept. 496, 1935.

[7] Halfman, R., "Experimental Aerodynamic Derivates of a Sinusoidally Oscillating Airfoil in Two-dimensional Flow," NACA TN 2465, 1951.

[8] Mertens, C., Pineda, S., Agate, M., Little, J. Fasel H., and Gross, A., "Effects of Structural Motion on the Aerodynamics of the X-56A Airfoil,", 54th AIAA Aerospace Sciences Meeting 4-8 January 2016, San Diego, California, USA, AIAA Paper 2016-2073, 2016.

[9] Leishman, G. J., "Challenges in Modeling the Unsteady Aerodynamics of Wind Turbines," in 21st ASME Wind Energy Symposium and the 40th AIAA Aerospace Sciences Meeting, Reno, NV, AIAA Paper 2002-0037, 2002.

[10] Leishman, G. J., and Baddoes, T. S., "A Semi-Empirical Model for Dynamic Stall," *Journal of the American Helicopter Society,* vol. 34, no. 3, 1989, pp. 3–17.

[11] Babu, A. V. S., Ramesh K., and Gopalarathnam, A., "Model Reduction in Discrete Vortex Methods for 2D Unsteady Aerodynamic Flows," in 34th AIAA Applied Aerodynamics Conference, AIAA AVIATION Forum, AIAA paper 2016-4163, Washington, D.C., 2016.

[12] Cleaver, D. J., Wang, Z., and Gursul, I., "Bifurcating Flows of Plunging Airfoils at High Strouhal Numbers," *Journal of Fluid Mechanics,* vol. 708, pp. 349-376, 2012. doi: https://doi.org/10.1017/jfm.2012.314

7

[13] Heathcote, S., "Flexible Flapping Airfoil Propulsion at Low Reynolds Numbers," Ph.D. Dissertation, Department of Mechanical Engineering, Univ. of Bath, Bath, England, U.K., 2006.

[14] Cleaver, D. J., Wang Z., and Gursul, I., "Vortex Mode Bifurcation and Lift Force of a Plunging Airfoil at Low Reynolds Numbers," 48th AIAA Aerospace Sciences Meeting, Orlando, Florida, AIAA Paper 2010-390, 2010.

[15] Schluter, J. U., "Lift Enhancement at Low Reynolds Numbers Using Pop-up Feathers," 39th AIAA Fluid Dynamics Conference, AIAA Paper 2009-4195, 2009.

[16] Sunada, S., Sakaguchi, A., and Kawachi, K., "Airfoil Section Characteristics at a Low Reynolds Number," *Journal of Fluids Engineering-Transactions of the ASME,* vol. 119, no. 1, 1997, pp. 129-135.

[17] Lee T., and Su, Y. Y., "Low Reynolds number airfoil aerodynamic loads determination," *Experiments in Fluids,* vol. 53, 2012, pp. 1177–1190.

[18] Laitone, E. V., "Wind tunnel tests of wings at Reynolds numbers below 70 000," *Experiments in Fluids,* vol. 23, 1997, pp. 405-409.

American Institute of Aeronautics and Astronautics
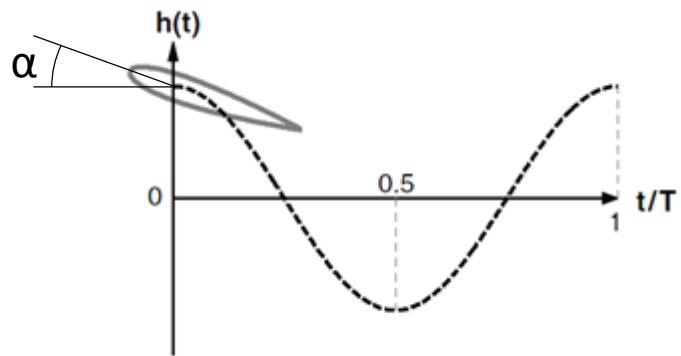
Figure 1. Plunging motion.

American Institute of Aeronautics and Astronautics

a)

b)
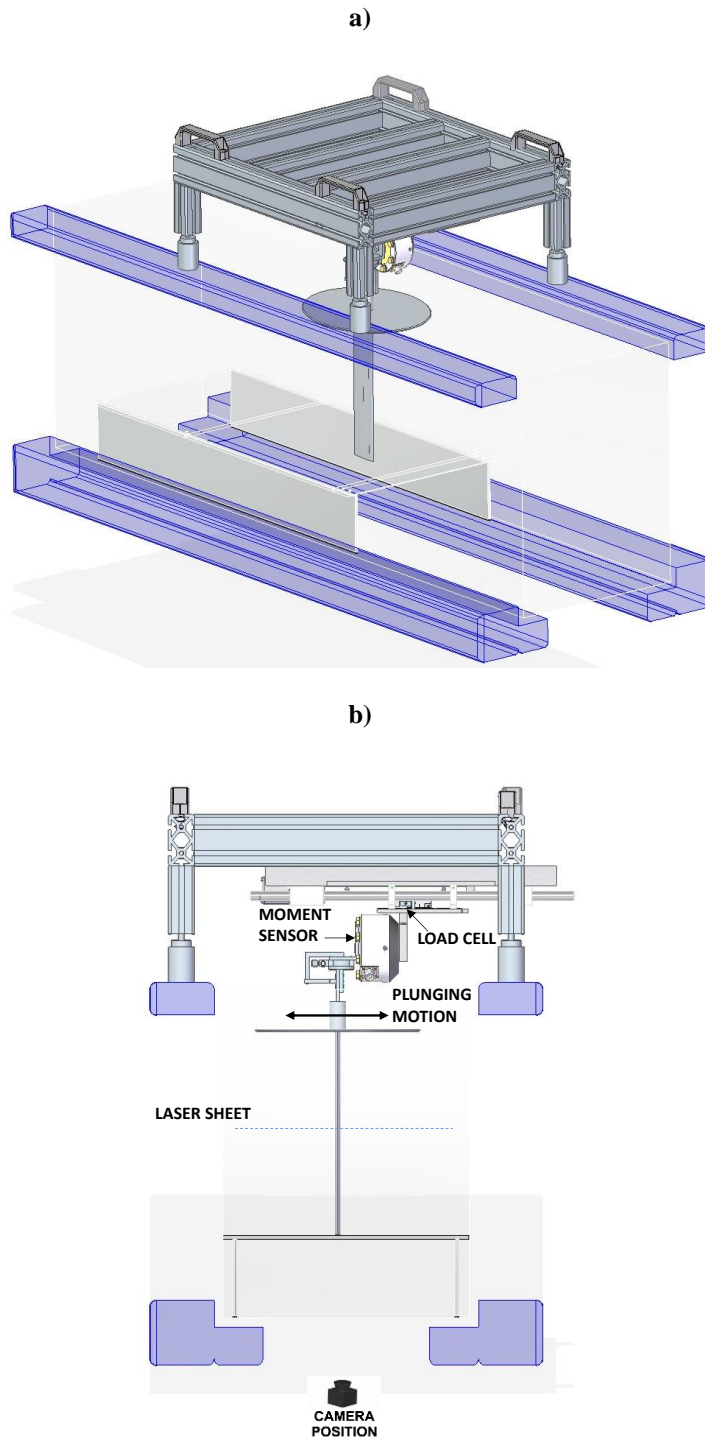
Figure 2. Test rig a) isometric view and b) front view.
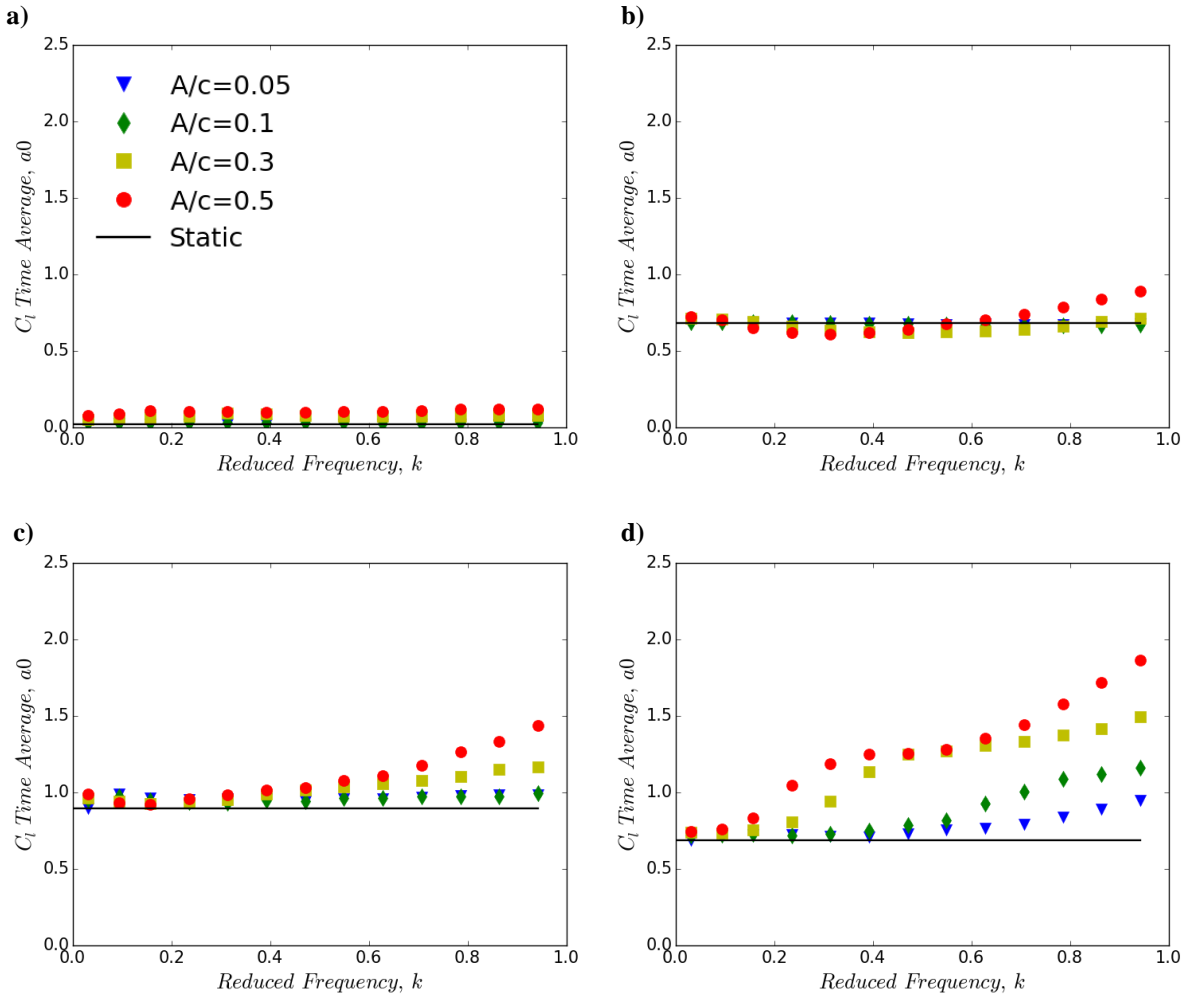
American Institute of Aeronautics and Astronautics
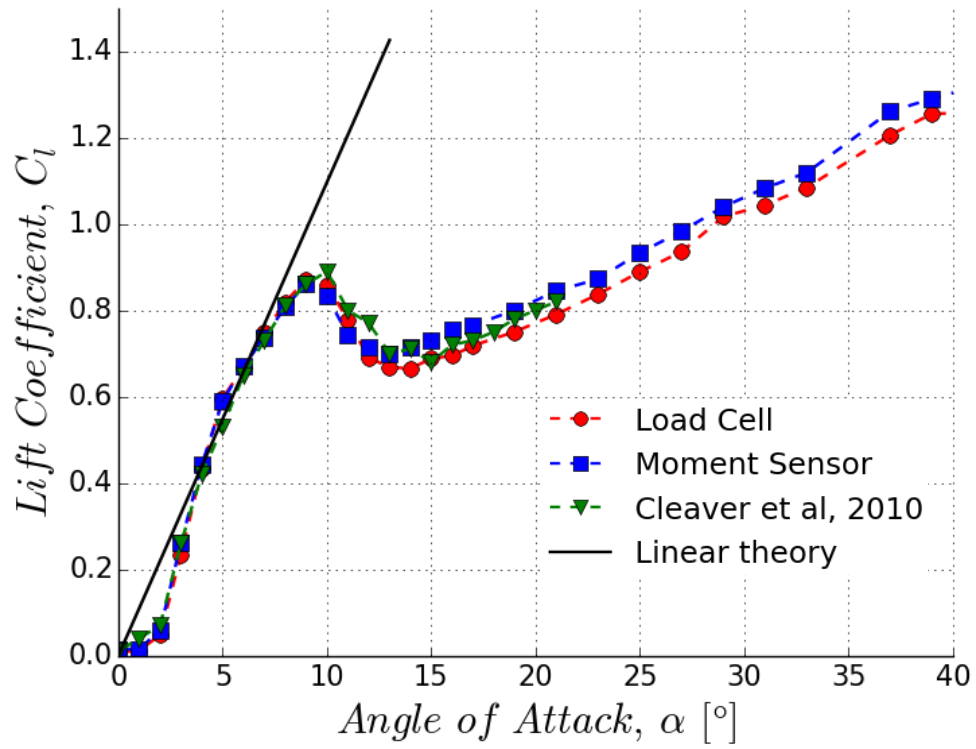
Figure 3. Lift measurements for stationary airfoil. Load cell (red circle), lift from moment sensor (blue square), Cleaver *et al*. [14] (green triangle), linear theory (2π*a*) (black line).
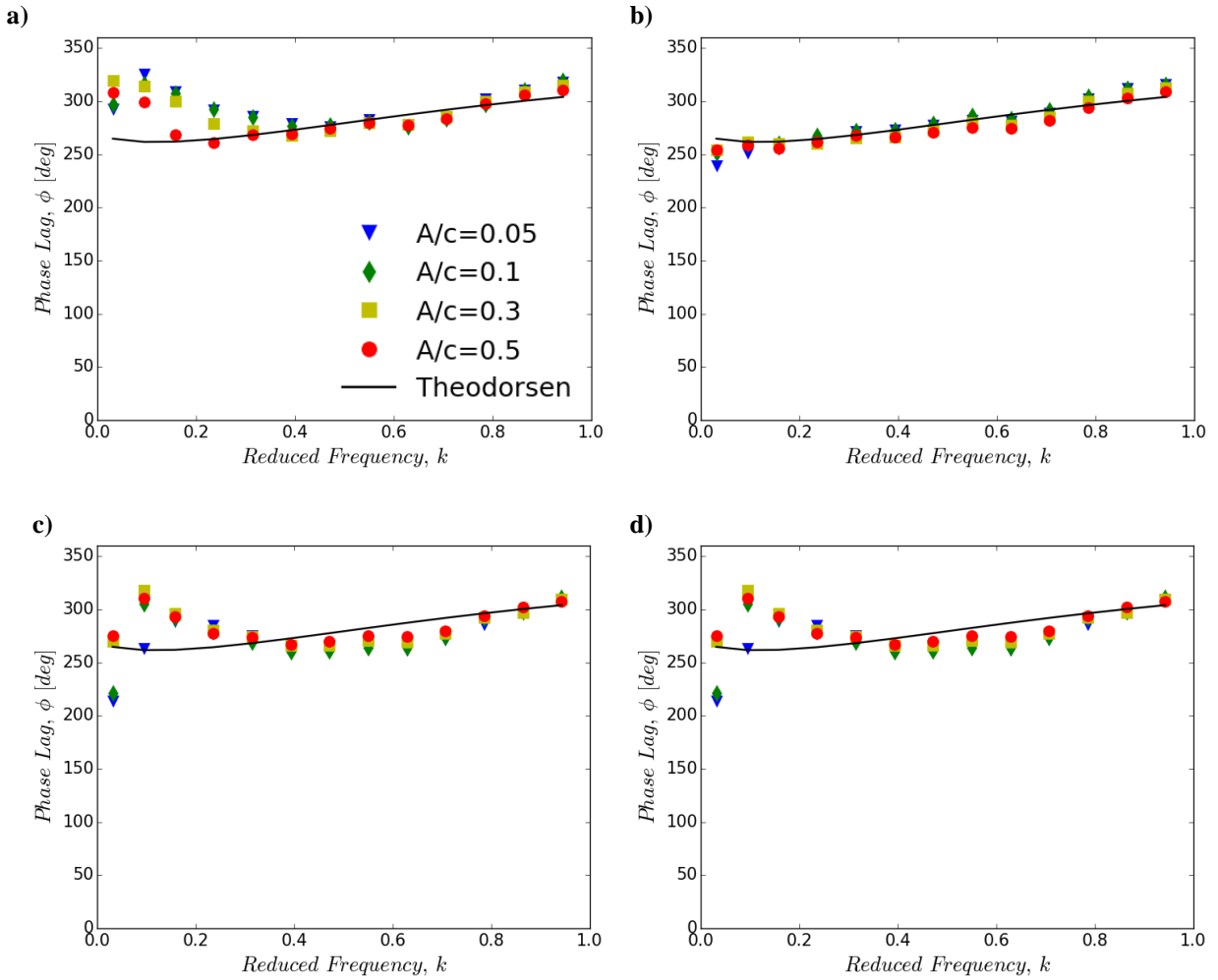
American Institute of Aeronautics and Astronautics

Figure 4. Time-averaged lift as a function of the plunging reduced frequency k and amplitude A/c. a) $\alpha=0°$, b) $\alpha=5°$, c) $\alpha=9°$, d) $\alpha=15°$.
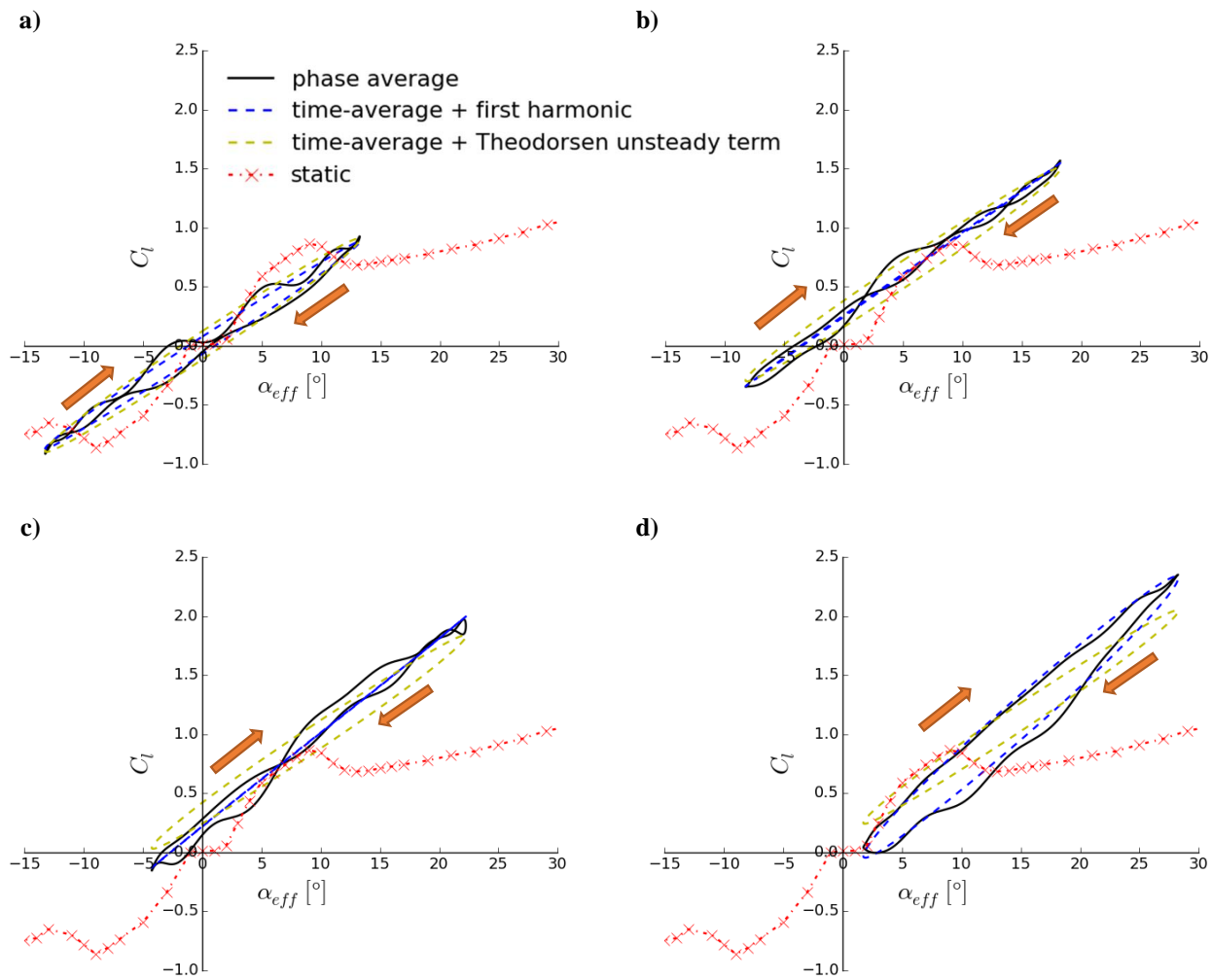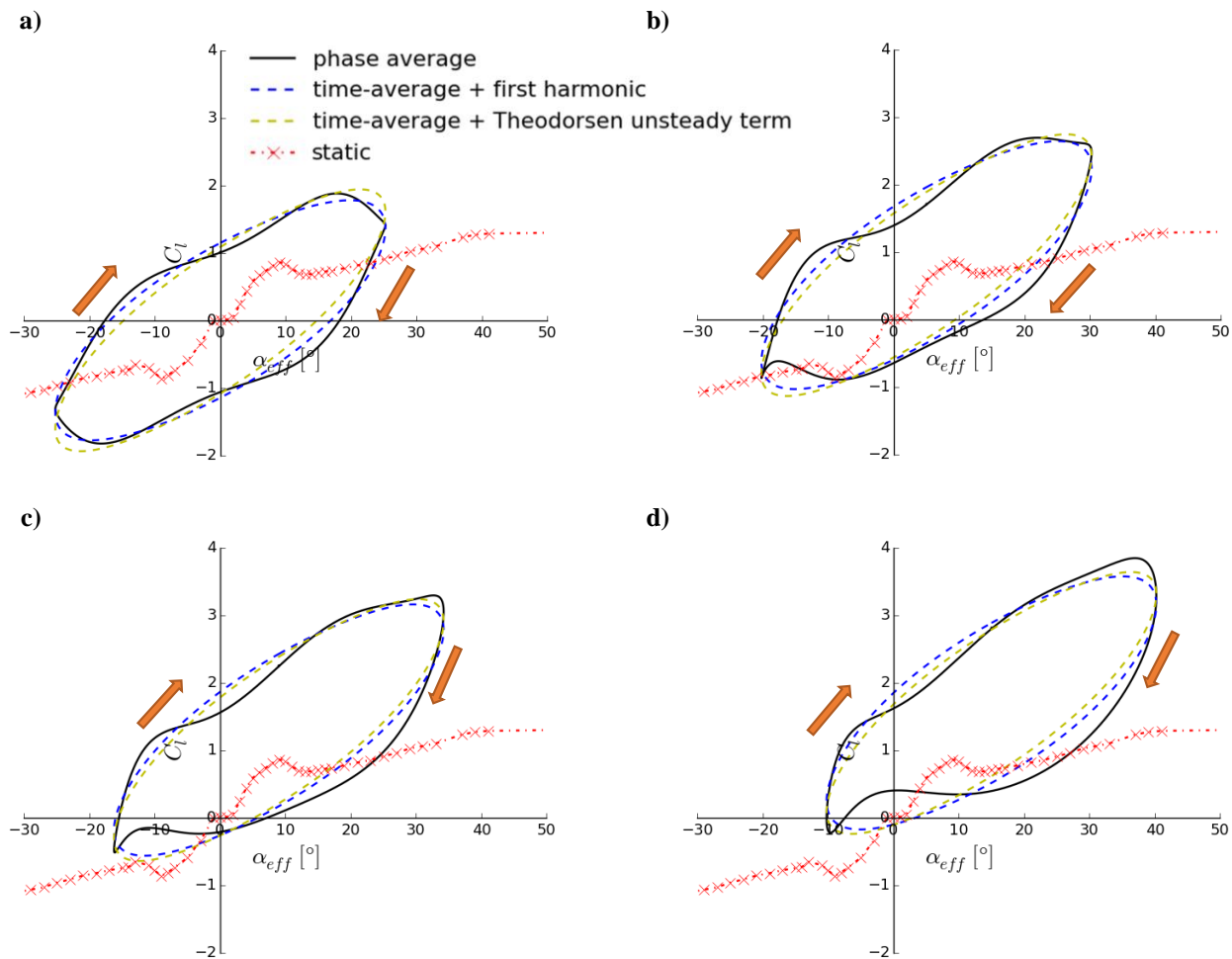
American Institute of Aeronautics and Astronautics
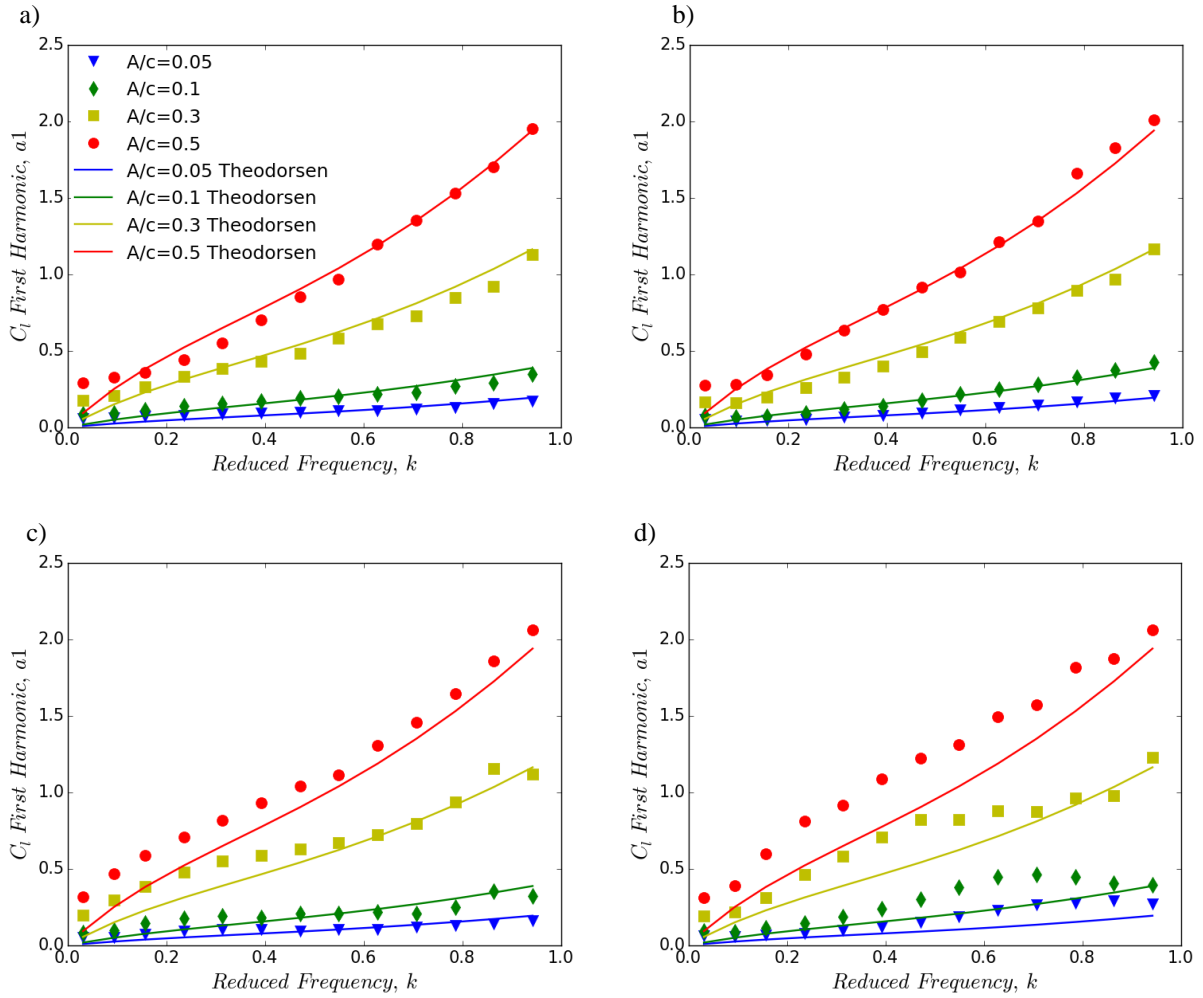
Figure 5. First harmonic of lift oscillation as a function of the plunging reduced frequency k and amplitude A/c. a) α=0°, b) α=5°, c) α=9°, d) α=15°.

American Institute of Aeronautics and Astronautics
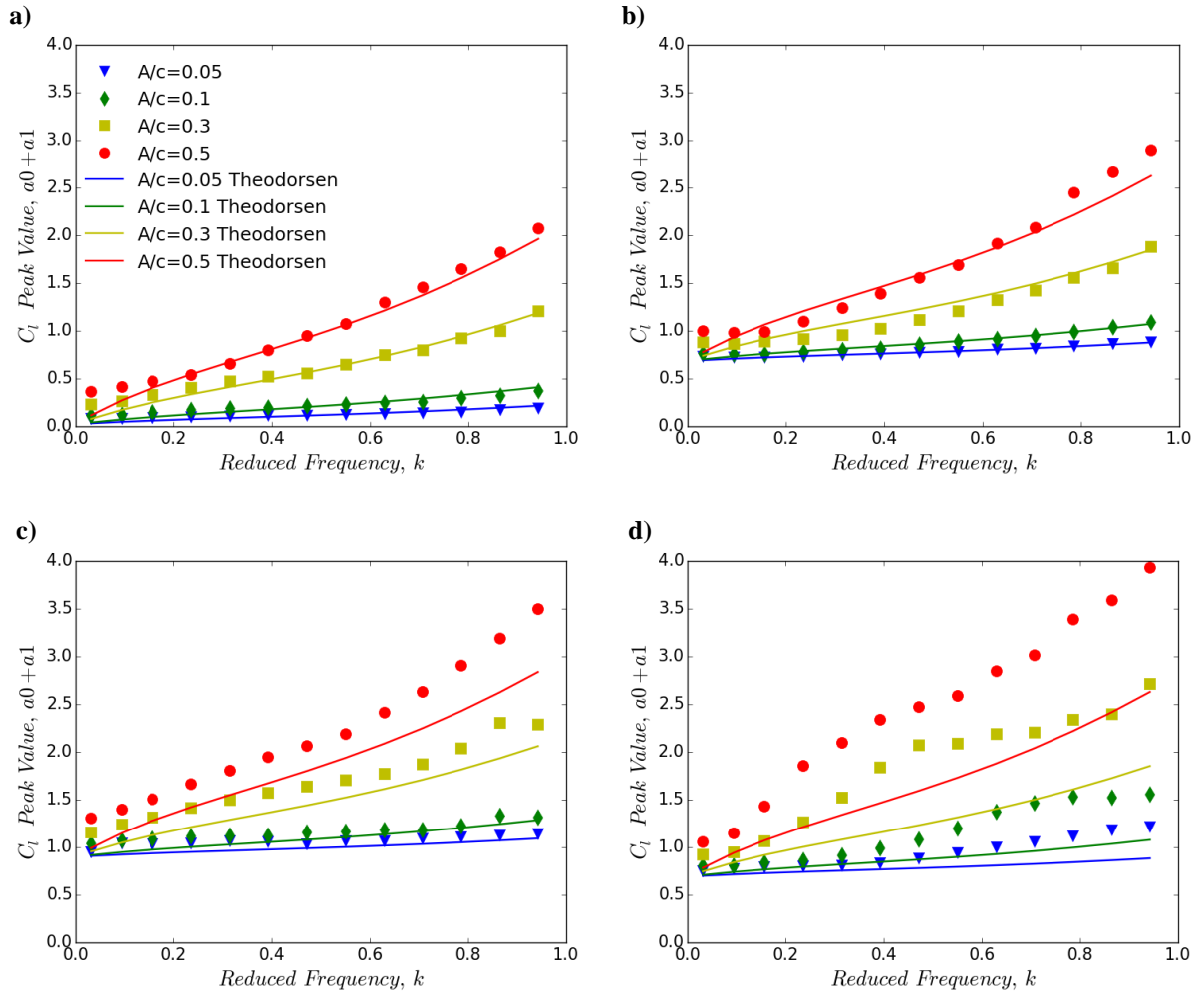
Figure 6. Peak value of lift oscillation as a function of the plunging reduced frequency k and amplitude A/c. a) α=0°, b) α=5°, c) α=9°, d) α=15°.

American Institute of Aeronautics and Astronautics

Figure 7. Phase lag of lift variation as a function of the plunging reduced frequency k and amplitude A/c. a) α=0°, b) α=5°, c) α=9°, d) α=15°.

American Institute of Aeronautics and Astronautics

Figure 8. Phase-averaged lift against effective angle of attack for plunging reduced frequency k**=0.47 and amplitude** A/c**=0.5. a)** α**=0°, b)** α**=5°, c)** α**=9°, d)** α**=15°. The arrow indicates the direction of the plunging motion.**

16

American Institute of Aeronautics and Astronautics

Figure 9. Phase-averaged lift against effective angle of attack for plunging reduced frequency *k*=0.94 and amplitude *A/c*=0.5. a) α=0°, b) α=5°, c) α=9°, d) α=15°. The arrow indicates the direction of the plunging motion.
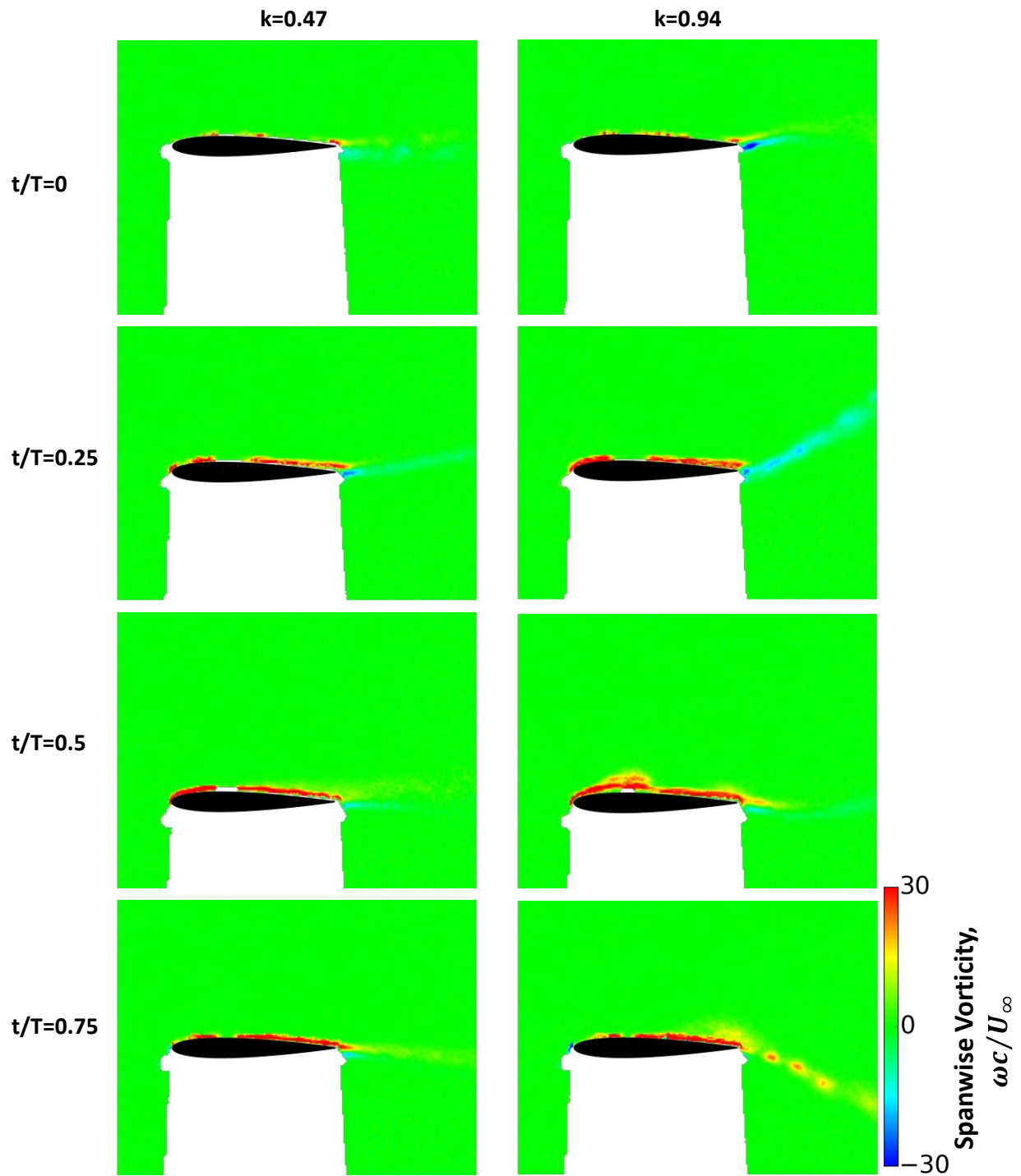
American Institute of Aeronautics and Astronautics

Figure 10.   **Phase-averaged contour plot of spanwise vorticity for α=0°: *k*=0.47 (left), *k*=0.94 (right).**
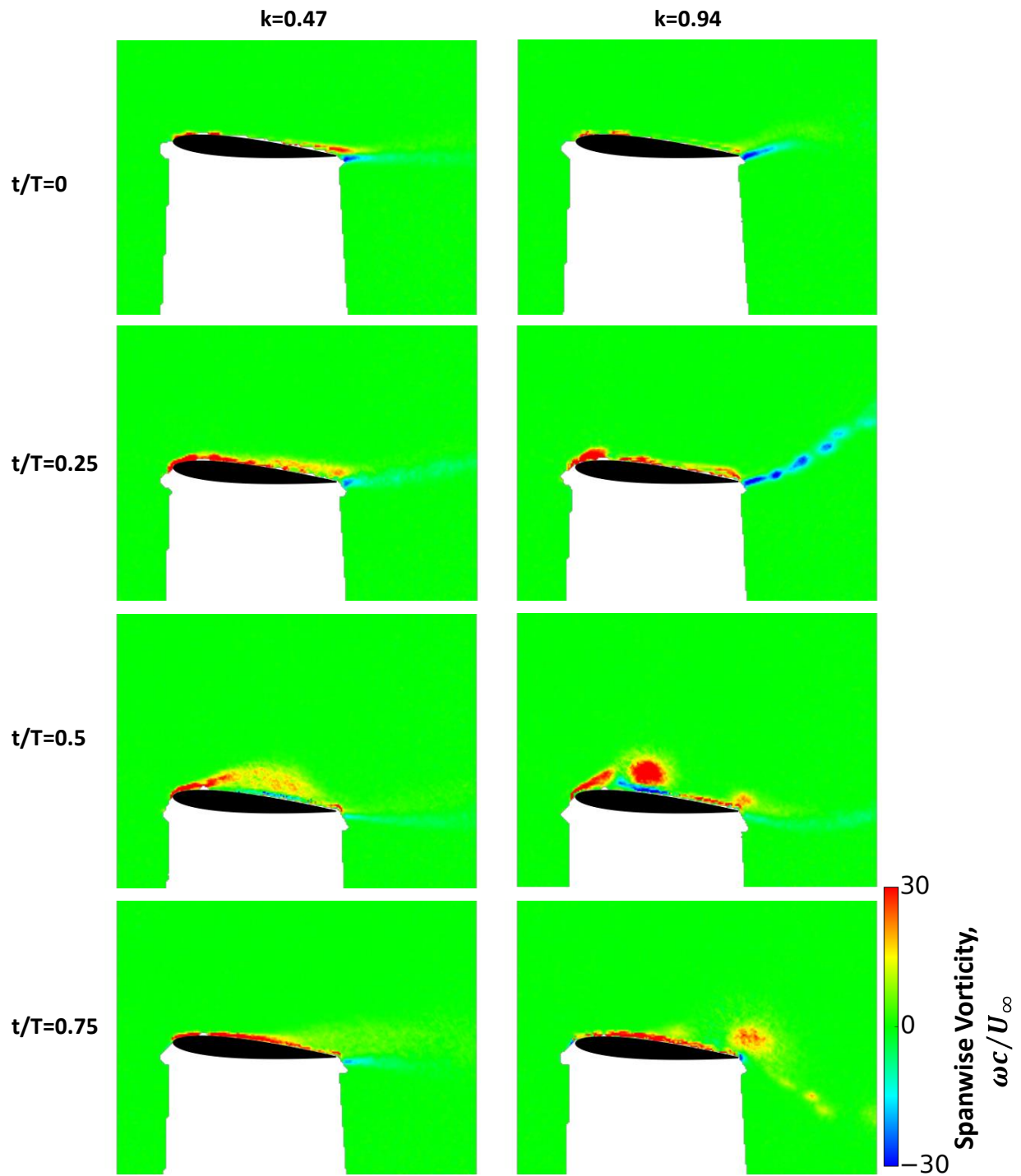
Figure 11. Phase-averaged contour plot of spanwise vorticity for $\alpha=5°$: $k=0.47$ (left), $k=0.94$ (right).

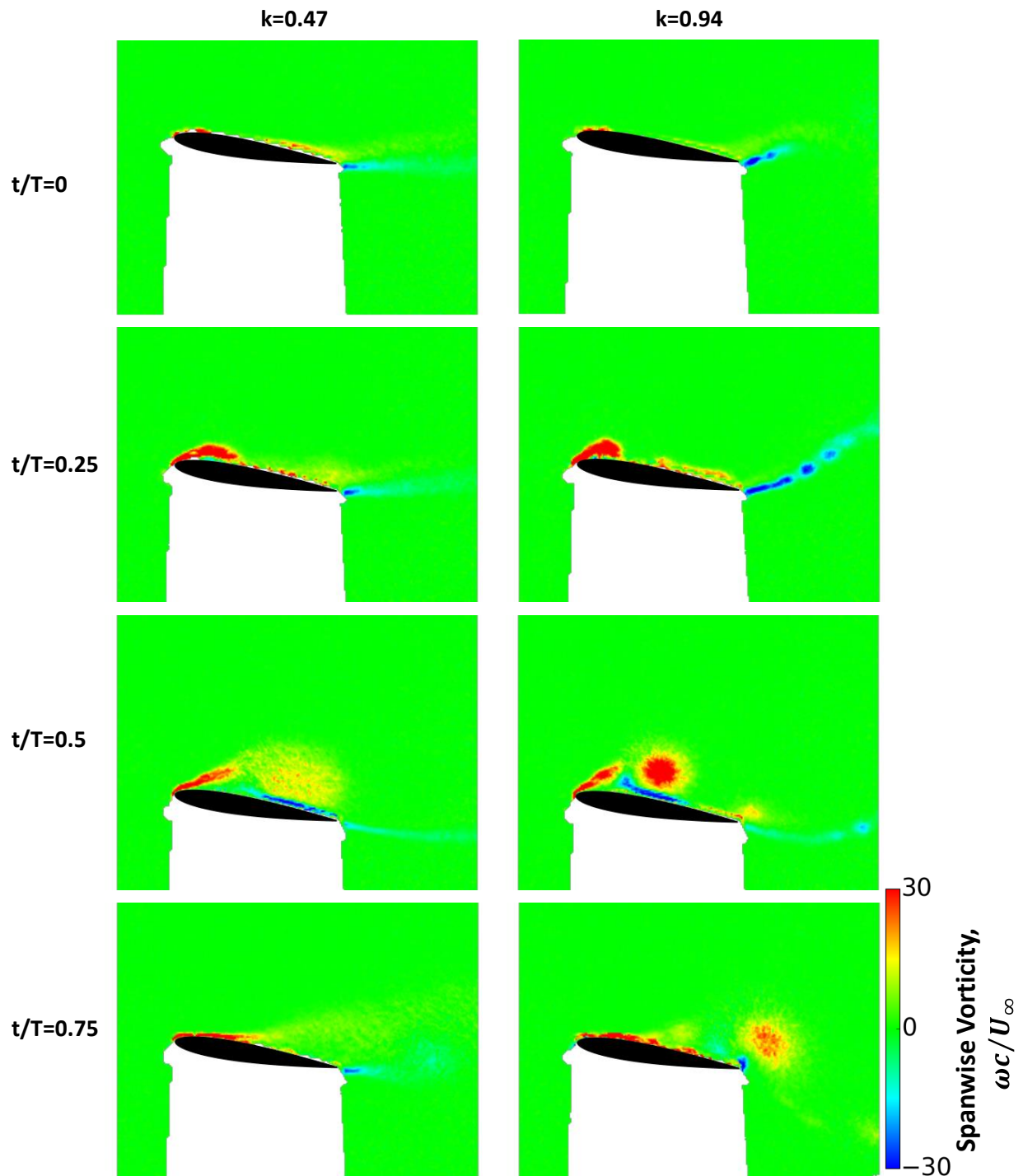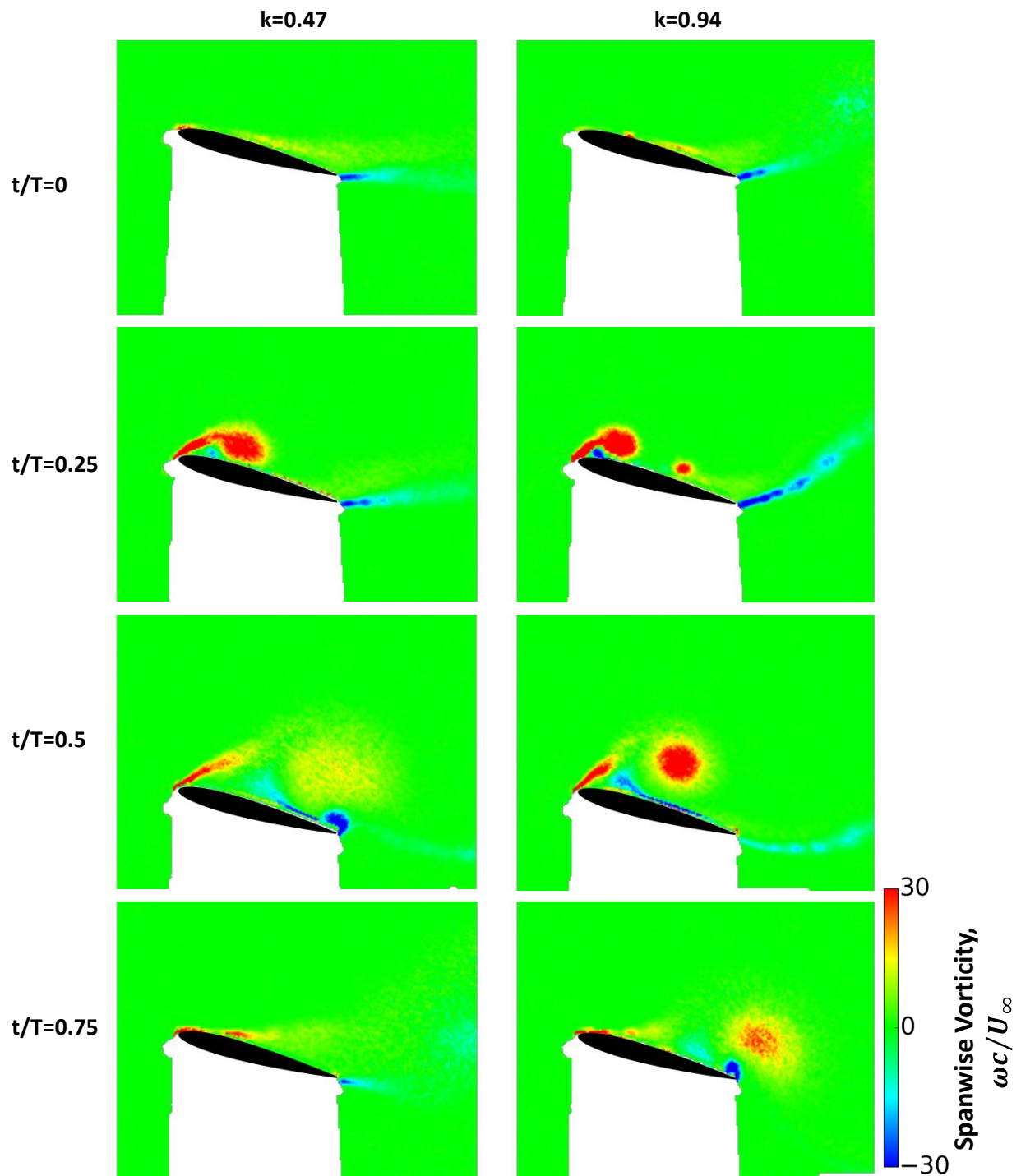**Figure 12.** Phase-averaged contour plot of spanwise vorticity for $\alpha=9°$: $k=0.47$ (left), $k=0.94$ (right).

American Institute of Aeronautics and Astronautics

Figure 13. Phase-averaged contour plot of spanwise vorticity for α=15°: *k*=0.47 (left), *k*=0.94 (right).

American Institute of Aeronautics and Astronautics